

# Automatic Symmetry-integrated Brain Injury Detection in MRI Sequences

Yu Sun<sup>1</sup>, Bir Bhanu<sup>1</sup>, Shiv Bhanu<sup>2</sup>

1. Center for Research in Intelligent Systems, University of California, Riverside, CA 92521.
2. School of Medicine, University of California, San Francisco, CA 94122.  
ysun@ee.ucr.edu, bhanu@ee.ucr.edu, shiv.bhanu@ucsf.edu

## Abstract

*This paper presents a fully automated symmetry-integrated brain injury detection method for magnetic resonance imaging (MRI) sequences. One of the limitations of current injury detection methods often involves a large amount of training data or a prior model that is only applicable to a limited domain of brain slices, with low computational efficiency and robustness. Our proposed approach can detect injuries from a wide variety of brain images since it makes use of symmetry as a dominant feature, and does not rely on any prior models and training phases. The approach consists of the following steps: (a) symmetry integrated segmentation of brain slices based on symmetry affinity matrix, (b) computation of kurtosis and skewness of symmetry affinity matrix to find potential asymmetric regions, (c) clustering of the pixels in symmetry affinity matrix using a 3D relaxation algorithm, (d) fusion of the results of (b) and (c) to obtain refined asymmetric regions, (e) Gaussian mixture model for unsupervised classification of potential asymmetric regions as the set of regions corresponding to brain injuries. Experimental results are carried out to demonstrate the efficacy of the approach.*

## 1. Introduction

Magnetic resonance imaging (MRI) is a medical imaging technique most commonly used in radiology to visualize the structure and function of the body. It provides detailed images of the body in any plane with higher discrimination than other radiology imaging methods such as CT, SPECT, etc. Specifically, mining of brain injuries that appear in an MRI sequence is an important task that assists medical professionals to describe the appropriate treatment. Traditionally, the boundary or region of an injury in magnetic resonance imaging is usually traced by hand. This manual approach is time consuming, subjective and error prone. The computer-aided diagnosis on brain MRI reduces the manual workload by a combination of image processing and pattern recognition techniques. An efficient injury detection algorithm is important for diagnosis, planning and treatment. Currently in many computer-aided

applications, automatic or semi-automatic image segmentation or detection methods are recommended for clinical treatment that can significantly reduce the time and make such methods practical. Previous works [1-6], based on 2D and 3D image analysis, detect brain injuries reasonably well by using training sets and prior models, as well as using efficient preprocessing like registration, with injury boundary outlined. Numerous features are used in model matching schemes, like image intensity, texture, shape, etc. In this paper, *symmetry* is integrated with image analysis as a new kind of feature. The integration allows fully automatic brain injury detection, without training and prior modeling, and it is applicable to a wider range of MRI data with different ages and injury characteristics.

The rest of this paper is organized as follows. In section 2, we give an overview of related work and our contributions. In section 3, the technical details of our work are provided. Section 4 gives experimental results. Finally, conclusions are given in section 5.

## 2. Related Works and Our Contributions

### 2.1. Related Works

There are many challenges associated with automated detection of brain injuries. The brain injuries are always different in size, shape, and may appear in any location with different image intensities. Some injuries also deform other normal and healthy tissue structures. In order to solve those challenges, state-of-the-art region-of-interest (ROI) extraction techniques basically use two kinds of methods: tissue classification/segmentation and abnormality extraction. The tissue classification approach [1, 2] starts with brain segmentation based on a prior model of tissue, and extracts ROIs from classified clusters. Unfortunately, in order to obtain satisfactory classification results, large amounts of training data or a complex prior model is required, and the range of application is strictly restricted by the domain of training phase. The abnormality/target extraction approach [3, 4] generally builds a stochastic model for normal brain tissues, and simultaneously detects abnormality that is not a well fit into the model. However, it

Table 1. Comparison of related symmetry integration methods and this paper

| Authors                           | Principle of Techniques  | Datasets and Results  | Comments  |
|-----------------------------------|--|---|---|
| Saha et al. [12]                  | Brain MRI segmentation using a fuzzy point symmetry based genetic clustering technique.  | <i>Datasets:</i> Totally 181 MRI slices, shows seven slices in results.<br><i>Results:</i> Segmentation results in 2D; <i>Minkowski Score</i> to measure the quality of clustering compared with ground-truth.  | + Assignment of points to clusters in genetic algorithm by point symmetry based distance rather than Euclidean distance; no <i>a priori</i> info.<br>- Time consuming; many noisy regions in results; cope with internal symmetry within a region only.   |
| Bergo et al. [13]                 | MRI segmentation based on the analysis of texture symmetry.  | <i>Datasets:</i> Five images from five patients.<br><i>Results:</i> Lesion segmentation results in 2D and 3D, with ground-truth.  | + Not rely on a template; good generality; enhance texture symmetry.<br>- Not robust to changes in parameters; uses only local symmetry.  |
| Ray et al. [14]                   | Locate brain abnormality by finding a bounding box around it using the symmetry analysis.  | <i>Datasets:</i> Six images - no source.<br><i>Results:</i> Abnormality detection results in 2D; no ground-truth; <i>Dice Coefficient</i> to measure the abnormality detection performance.   | + No registration; no training image; can be implemented in real-time.<br>- Need the reference (template) image; abnormality boundary in segmentation result is not well outlined.  |
| Sun, Bhanu and Bhanu - This paper | Detect brain injury in MRI by symmetry integration in several steps associated with segmentation, clustering and classification. | <i>Datasets:</i> MRI sequences of 2 patients, with 16 slices for each; shows results on 4 slices of each patient;<br><i>Results:</i> Both segmentation and injury detection results in 2D with ground-truth; <i>Error rate</i> to measure the detection accuracy compared to ground-truth in 2D and 3D. | + Integrates symmetry in all steps; no prior model or template; no training data; good generality; efficient segmentation algorithm; uses global symmetry rather than local or internal symmetry.<br>- Some very low contrast injured regions are missed. |

is always challenging to build a complete prior model in order to cover enough tissue information. Another abnormality extraction method is called digital subtraction [5], which is useful to track structure or volume changes of brain collected at different times. The accurate subtraction relies highly on normalization and registration [6]. As a result, most of the current ROI extraction methods highly depend on the quality of preprocessing and prior knowledge. Our method overcomes the above limitations to a great extent by integrating symmetry information in segmentation and abnormality extraction.

## 2.2. Our Contributions

Related works in [12, 13, 14] basically integrate symmetry information into brain MRI segmentation in only a single step, whereas our method integrates symmetry in all the steps of segmentation, clustering and classification in the whole system. The limitations of these techniques compared to our method are shown in Table 1. We formulate the proposed new idea based on the observation that for most abnormality detection methods, though different in principle, accept a common criterion that abnormal regions are detected by their properties that deviate from the expected normal and healthy tissue

properties. Specified to our case, since most of the injuries are asymmetric with their mirror regions against the symmetry axis, while the other healthy brain structures are highly symmetric, we are able to detect injuries by symmetry integration. Therefore, asymmetry is regarded as a distinct property of injuries that deviates from other normal symmetric tissues. By integrating symmetry, we overcome the limitations of other approaches and this paper makes following contributions:

- (a) By symmetry integration, our method does not need prior models for injury detection. We eliminate symmetric tissues without further classifying them by a large amount of training data. Furthermore, symmetry information is able to classify brain image into symmetric and asymmetric regions, and our results show that the extracted asymmetric regions cover almost all injuries or other abnormalities.
- (b) Unsupervised classification can be used to classify asymmetric regions into injuries and other normal regions by features composed of image intensities and 3D brain asymmetry volumes, without preprocessing and training.
- (c) Our method integrates symmetry information in almost all steps in approach, whereas other works only integrate symmetry in single step.

### 3. Technical Approach

The overall diagram of our method, with example results of each step, is shown in Fig. 1. Since symmetry is the most important feature in our method, we integrate symmetry in several steps that can be seen in Fig 1:

- (1) Symmetry affinity matrix computation in Fig 1(b);
- (2) Symmetry-integrated image segmentation in Fig 1(c);
- (3) Asymmetric region extraction by kurtosis and skewness of symmetry affinity, as in Fig 1(d);
- (4) Cluster and identify asymmetric groups in Fig 1(e) (f).
- (5) Classify asymmetric regions into injury and non-injury using intensity and 3D asymmetry volume as in Fig 1(h).

In step (1), a symmetry affinity matrix is obtained, that is used frequently as a measurement of symmetry in later steps. Step (2) enhances symmetry level of segmentation results to make sure that most symmetric parts are segmented appropriately. Thus it prevents misclassification of symmetric parts into asymmetric regions in a later step. In step (3), kurtosis and skewness of symmetry affinity matrix are computed and they are used to extract asymmetric regions from segmented parts. Meanwhile in step (4), symmetry affinity matrix is also used for clustering and identification of asymmetric groups. Results from step

(3) and (4) are fused to obtain refined asymmetric regions in Fig 1(g). Finally, an unsupervised classifier is used to extract injuries from the asymmetric regions.

#### 3.1. Symmetry Extraction and the Symmetry Affinity Matrix

In order to integrate symmetry, a symmetry measurement scheme of MRI image is needed. We use global symmetry constellations of features [7] to detect the reflective symmetry axis for the brain, as in Fig 1(a). A symmetry affinity matrix as in Fig 1(b), measuring the symmetry level of each pixel with respect to its symmetry counterpart pixel reflected by the axis, is computed by curvature of gradient vector flow (CGVF) [8]:

$$Curv(x,y) = \frac{1}{|V|^3} [(v_x + u_y)uv - u_x v^2 - v_y u^2] \quad (1)$$

Let the GVF of image be:

$$V = [u(x,y), v(x,y)] \quad (2)$$

In equation (1),  $u_x = \partial u / \partial x$ ,  $u_y = \partial u / \partial y$ ,  $v_x = \partial v / \partial x$ ,  $v_y = \partial v / \partial y$  are the first derivatives of pixel along x and y

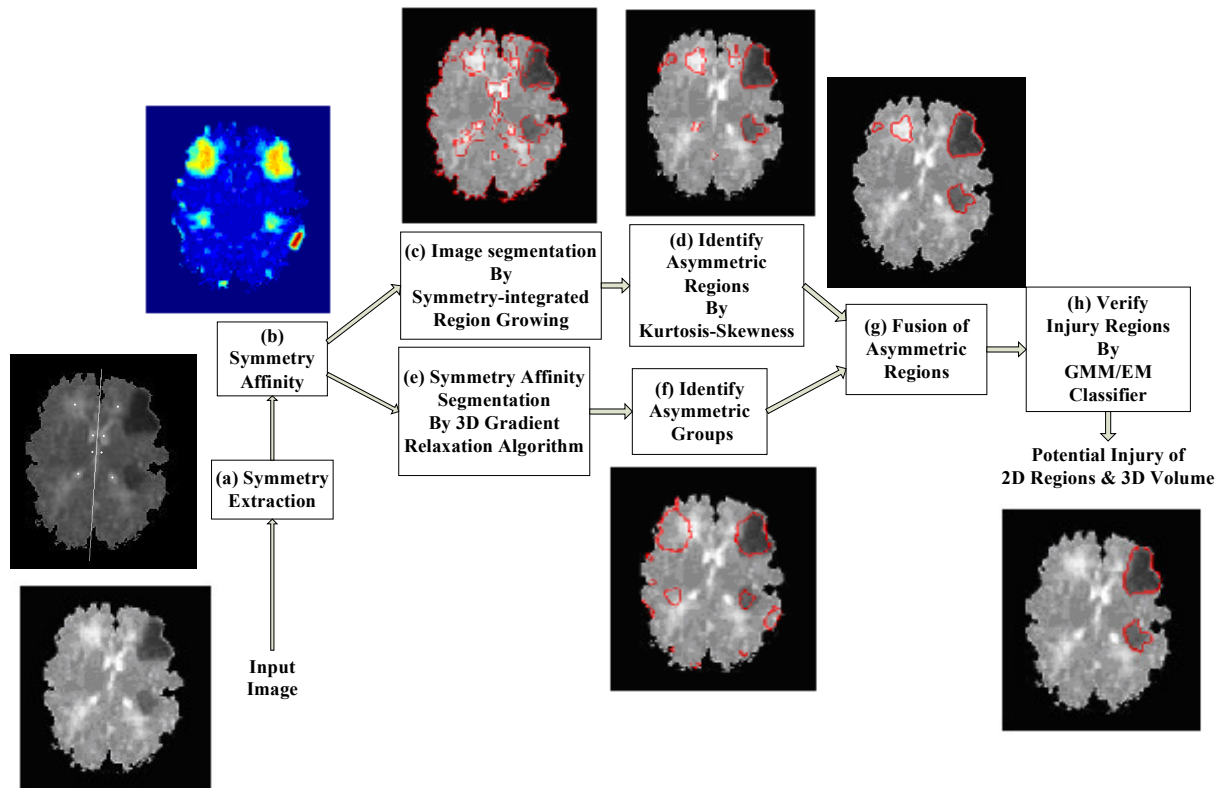


Fig 1. Overall system diagram

directions. Considering a pixel  $(x_i, y_i)$ , we define its symmetry affinity as:

$$C(x_i, y_i) = |Curv(x_i, y_i) - Curv(x_j, y_j)| \quad (3)$$

where  $(x_j, y_j)$  is the symmetric counterpart of  $(x_i, y_i)$  by the symmetry axis. If the two points have locally symmetric fields, then values of  $Curv(x_i, y_i)$  and  $Curv(x_j, y_j)$  should be closer. Three other symmetry conditions are stated in [8], which can be combined with eq. (3) to build the affinity matrix. The brighter regions in symmetry affinity matrix indicate potential asymmetric fields in the image. The symmetry affinity matrix is further used to outline the symmetry constraint for pixel aggregation in a region growing approach for image segmentation in the next subsection.

### 3.2. Symmetry-integrated Image Segmentation

Region growing segmentation accepts image intensity as a constraint for pixel aggregation, either by color or gray scale. Recent improvements in constraint include a combination of texture, shape, etc., to segment regions with different properties. In order to make sure that symmetric parts are segmented appropriately, in our work, a symmetry constraint derived from symmetry affinity matrix is integrated into region growing constraint as shown below:

$$\delta_{\text{symmetry}}(i, j) = \frac{\frac{\pi}{2} + \text{actan}(\sqrt{(1+C_i)(1+C_j)})}{\pi} + \frac{1 + |\sqrt{C_i} - \sqrt{C_j}|}{2} \quad (4)$$

$C_i$  and  $C_j$  in equation (4) are symmetry affinities of pixel  $i$  and neighboring region  $j$ . Equation (4) provides the following symmetry constraints: the first term controls the symmetry level, which means that if both patterns  $i$  and  $j$  indicate low symmetry affinities (highly symmetric), they are more likely to be aggregated by decreasing the constraint; while the second term favors more similar symmetry affinities. In our work, the symmetry constraint is combined with gray scale intensity and texture to build an aggregation constraint as follows:

$$\delta(i, j) = \delta_{\text{symmetry}}(i, j) + \delta_{\text{gray}}(i, j) + \delta_{\text{texture}}(i, j) \quad (5)$$

where  $\delta_{\text{gray}}(i, j)$  uses the intensity difference of  $i$  and  $j$  as gray-level constraint, and  $\delta_{\text{texture}}(i, j)$  uses texture difference, obtained by Gabor filter, as the texture constraint. Based on the aggregation constraint, pixel  $i$  will be aggregated into the neighboring region  $j$  if constraint  $\delta(i, j)$  between them is below a threshold  $\delta_m$ . We call equation (5) as the symmetry integrated multiple constraints. After segmentation, regions with natural symmetric properties will be segmented symmetrically. An example result is shown in Fig 1(c). This approach will improve the performance of asymmetric

region extraction in the next section. Note that Gupta et al. [10] applied symmetry integration (edge-weight) to enhance the symmetry level in a graph-cut segmentation approach. This integration has very limited improvements in segmentation results, compared to our method.

### 3.3. Asymmetric Region Extraction

A region growing algorithm with symmetry constraints for pixel aggregation separates symmetric and asymmetric parts in segmentation results by ensuring that naturally symmetric parts are segmented symmetrically. The asymmetric region extraction basically classifies the segmented regions into symmetric and asymmetric regions. We provide a new method using kurtosis and skewness of symmetry affinity matrix to detect asymmetric regions. For a sample of  $n$  values the sample kurtosis and skewness are given by equations (6) and (7):

$$\text{Kurtosis: } g_4 = \frac{\mu^4}{\delta_2^2} = \frac{\frac{1}{n} \sum_{i=1}^n (x_i - \bar{x})^4}{\left(\frac{1}{n} \sum_{i=1}^n (x_i - \bar{x})^2\right)^2} \quad (6)$$

$$\text{Skewness: } g_3 = \frac{\mu^3}{\delta_2^{1.5}} = \frac{\frac{1}{n} \sum_{i=1}^n (x_i - \bar{x})^3}{\left(\frac{1}{n} \sum_{i=1}^n (x_i - \bar{x})^2\right)^{1.5}} \quad (7)$$

Kurtosis is a measure of the "peakiness" of the probability distribution of a random variable. A larger kurtosis means that the probability distribution indicates a higher and narrower peak. Kurtosis property has been applied in image processing to detect the abnormality based on the reason that kurtosis measures the deviation of a distribution from the background [9]. We use kurtosis of symmetry affinity matrix to detect asymmetric regions, based on the observation that the asymmetric regions (brighter) in the symmetry affinity matrix can be regarded as abnormal targets with background, where symmetry affinity values of pixels are very low and smoothly distributed. For each segmented region the kurtosis of its symmetry affinity is computed using eq. (6), resulting in a single kurtosis value for each region. Larger kurtosis of a region means more deviation in its symmetry affinity distribution, which leads to potential asymmetry.

The skewness is another cue for asymmetry detection. Once we know the mean symmetry affinity value of a region, the negative skewness means that the distribution is left-tailed to the mean value. Since zero symmetry affinity means perfect symmetry, negative skewness means that the region affinity favors more asymmetry. The asymmetric region detection can be expressed as follows:

(a) Discard symmetric regions whose mean symmetry affinity is quite low; note that highly symmetric regions will have a low affinity.

(b) For each of the remaining regions, compute its kurtosis minus skewness combination  $g = (g_4 - g_3)$  from eq. (6) and (7), and build a histogram for the combination  $g$  of all candidate regions. Larger  $(g_4 - g_3)$  indicates a more asymmetric region. A threshold  $\Omega$  is found to partition the histogram into symmetric and asymmetric regions. Regions with values of  $(g_4 - g_3)$  larger than the threshold are extracted as asymmetric regions, as shown in Fig 1(d).

### 3.4. Symmetry Affinity Clustering

The purpose of asymmetric region extraction is to cover all the injured regions, while at the same time allowing the number of other normal asymmetric regions be as small as possible. The asymmetric regions obtained in the previous section can be combined with the results of symmetry affinity clustering to reduce the number of normal asymmetric regions. Symmetry affinity clustering is realized by 3D relaxation method based on maximizing a criterion function [11]. Basically this algorithm iteratively separates the symmetry affinity histogram into two classes, as symmetry and asymmetry. The original symmetry affinity valued between 0 and 1 is assigned as probability of each pixel. The mean neighborhood probability  $q_i$  of the  $i$ th pixel under consideration is denoted by the sum of the weighted symmetry affinities of its 8-neighborhood pixels from all slices at the same 2D neighborhood position, that build a 3D neighborhood. The mean 3D neighborhood probability  $q_i$  is shown as:

$$q_i(\lambda_k) = \frac{1}{8n} \sum_{j \in V_i} w_j p_j(\lambda_k) \quad (8)$$

where  $n$  is the number of slices in MRI sequence, and  $8n$  is the total number of pixels in 3D neighborhood  $V_i$ .  $p_j(\lambda_k)$  is equal to the symmetry affinity value of  $j$ th pixel in  $V_i$ , and  $w_j$  gives weight to each affinity of  $j$ th pixel, where less weight is assigned to pixels that belong to farther MRI slices. And the values of  $w_j$  satisfy the following two constraints:  $\sum w_j = 1$  and  $w_{j+1} = 0.5w_j$ . The first constraint ensures the normalization of the probability  $P_j$ , and the second constraint means that the weight of slice  $j+1$ , which is farther from the previous slice  $j$ , is half the value of slice  $j$ . The following iterative process will separate the distribution of symmetry affinity histogram into symmetry and asymmetry clusters, by updating symmetry affinity  $P_i$  of  $i$ th pixel:

$$p_i^{(n+1)}(\lambda_k) = p_i^{(n)}(\lambda_k) + \rho_i^{(n)}[q_i(\lambda_k) - 1] \quad (9)$$

where  $\rho_i$  in iteration  $n$  is updated as:

$$\rho_i^{(n)} = \begin{cases} \alpha_1 \rho_{i \max}^{(n)}, & \text{if } 2q_i(\lambda_1) - 1 > 0 \\ \alpha_2 \rho_{i \max}^{(n)}, & \text{if } 2q_i(\lambda_1) - 1 < 0 \end{cases} \quad (10)$$

and

$$\rho_{i \max}^{(n)} = \begin{cases} \frac{1 - p_i^{(n)}(\lambda_1)}{2q_i(\lambda_1) - 1}, & \text{if } 2q_i(\lambda_1) - 1 > 0 \\ \frac{p_i^{(n)}(\lambda_1)}{1 - 2q_i(\lambda_1)}, & \text{if } 2q_i(\lambda_1) - 1 < 0 \end{cases} \quad (11)$$

where  $\lambda_1$  means the cluster of asymmetry.  $\alpha_1$  and  $\alpha_2$  in eq. (10) are the control parameters constrained by  $\alpha_1 + \alpha_2 = 1$ , valued  $\alpha_1 = \alpha_2 = 0.5$  in our case. Normally, 2 iterations are enough to cluster symmetry and asymmetry pixels in symmetry affinity matrix, and the asymmetric clusters are shown in Fig 1(f).

The final asymmetric regions shown in Fig 1(g) are obtained by combing the results in Fig 1(d) and 1(f), by using the fact that the final asymmetric regions from 1(d) are extracted into 1(g) if the regions contain over 50% asymmetric pixels grouped by 1(f). That means if the two results (1(d) and 1(f)) have at least 50% overlap in common asymmetric fields, the regions in 1(d) are extracted as asymmetric regions into 1(g). The 50% overlap threshold is chosen by observation of results of a few testing slices, and it is found to be robust to MRI sequences. Lots of normal asymmetric regions are eliminated by this overlapping; at the same time all injuries or other abnormalities are reserved. Basically the result in Fig 1(g) contains all the injuries and the number of other normal asymmetric regions is minimized.

### 3.5. Injury Extraction

Asymmetric regions obtained from section 3.4 are potential candidates for extracting injuries. An unsupervised Expectation Maximization (EM) classifier with Gaussian Mixture Model (GMM) is used to classify candidate asymmetric regions into two classes: injury vs. non-injury, basically by a 2-dimensional feature, composed of gray scale intensity, and the 3D asymmetry volume. The 3D asymmetry volume is obtained by binarization of results in Fig 1(g), where the pixel belonged to asymmetric region is valued 1, and the pixel in other symmetric region is valued 0. The binary results of all slices in MRI sequence are added up to build the 3D asymmetry volume. The value of asymmetry volume means how frequently the asymmetric regions appear in slices at the same 2D position. If an injury exists in 3D MRI, its asymmetry in 2D slices will have a high value. Injuries are more likely to be classified into one group by using 3D asymmetry volume

feature. The mean value of 3D asymmetry volume of each asymmetric region in Fig 1(g) is used as a feature for classification, where the other feature is the mean gray scale value. The class with larger mean 3D asymmetry volume is identified as the injury class, and the final injury regions belonging to the injury class is shown in Fig 1(h).

## 4. Experimental Results

### 4.1. Datasets and Parameters

We use MRI datasets provided by Loma Linda University Medical Center at Loma Linda, CA. It is

composed of two sequences of MRI slices from two patients labeled as #A and #B. Sample slices are shown in Fig 2 and Fig 3. Slices in each MRI sequence are collected from 2D projections of different 3D brain layers for the same patient. Several challenging injury cases are also obtained from the Internet, and an example is shown in Fig 4. The 2 major parameters in our algorithm are: threshold  $\delta_i$  for region growing pixel aggregation criterion  $\delta(i, j)$  in equation (2), and the kurtosis-skewness histogram cut threshold  $\Omega$  for asymmetric region detection introduced in section 3.3. The values of the two parameters are 0.024 and 0.22 respectively. We use the same parameter setting for running all slices in all MRI sequences.

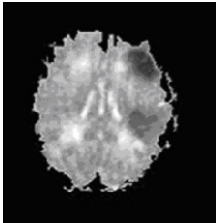
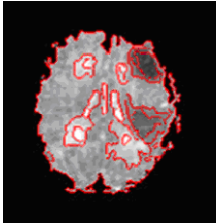
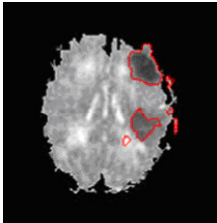
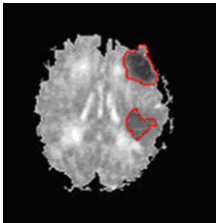
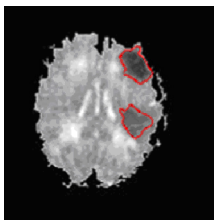
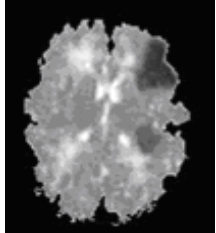
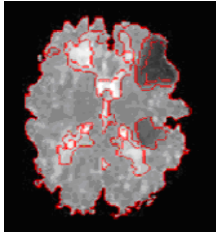
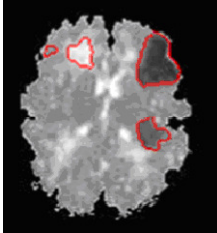
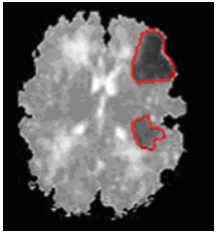
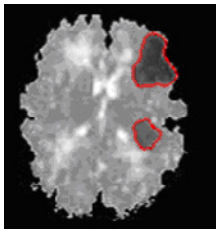
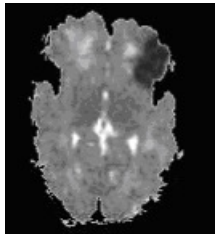
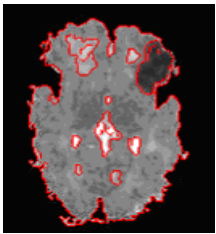
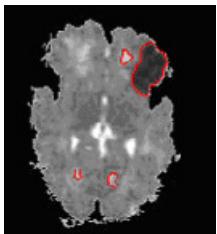
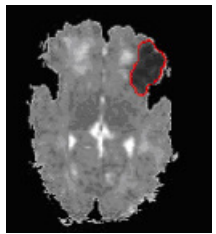
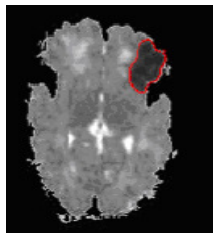
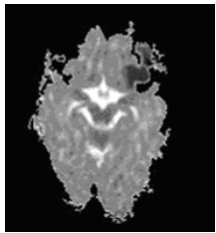
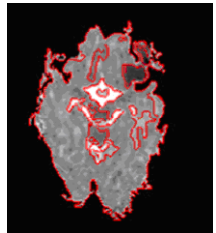
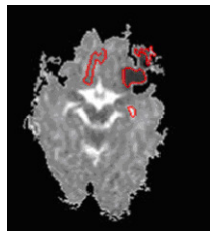
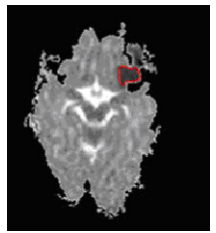
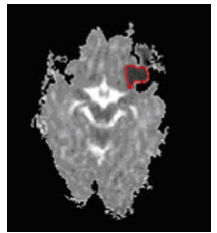
| MRI # | a. Original Image   | b. Segmentation   | c. Asymmetric Regions   | d. Injury Regions (Computed)   | e. Injury Regions (Ground-truth)  |
|-------|---|---|---|--|---|
| A6    |    |    |    |    |    |
| A7    |  |  |  |  |  |
| A9    |  |  |  |  |  |
| A11   |  |  |  |  |  |

Fig 2. Example results on slices for patient #A



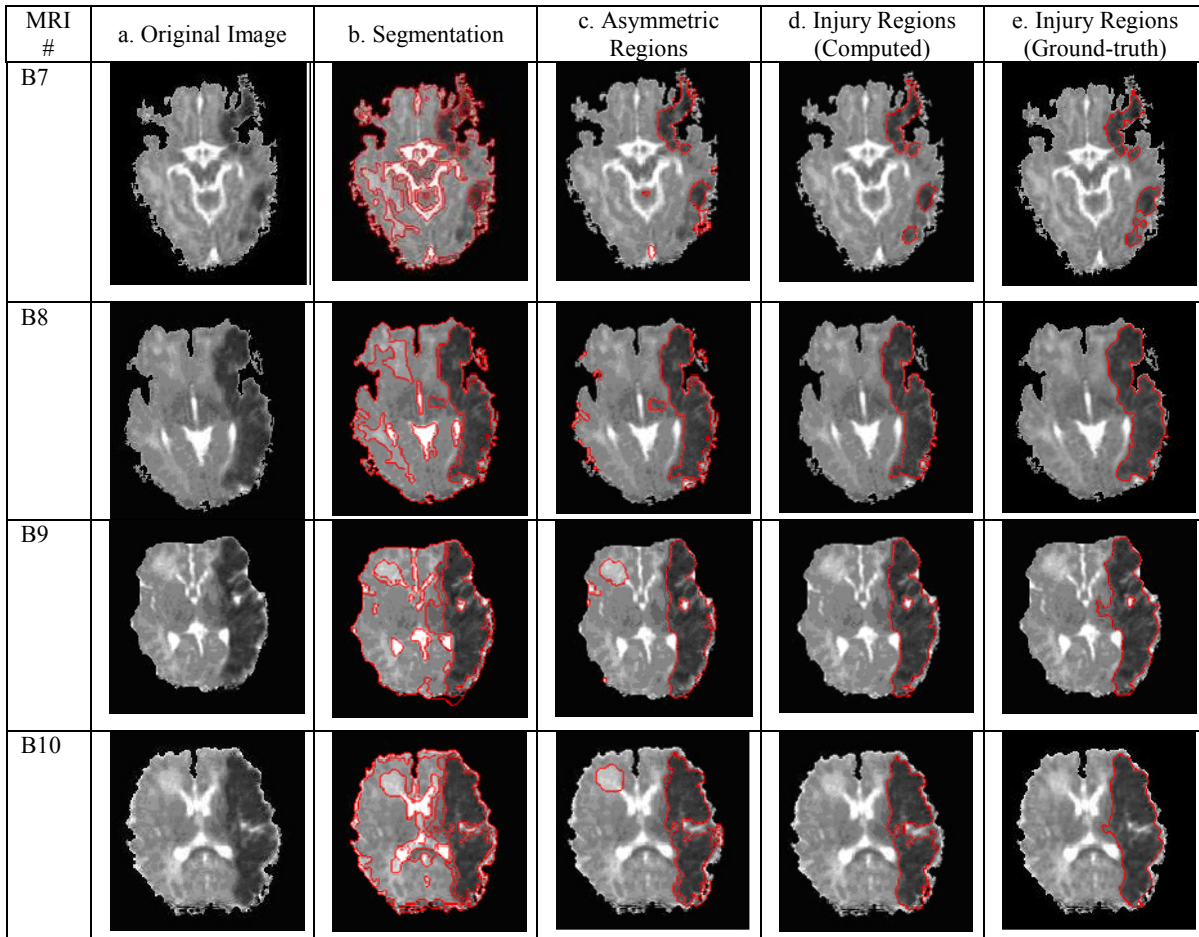


Fig 3. Example results on slices for patient #B

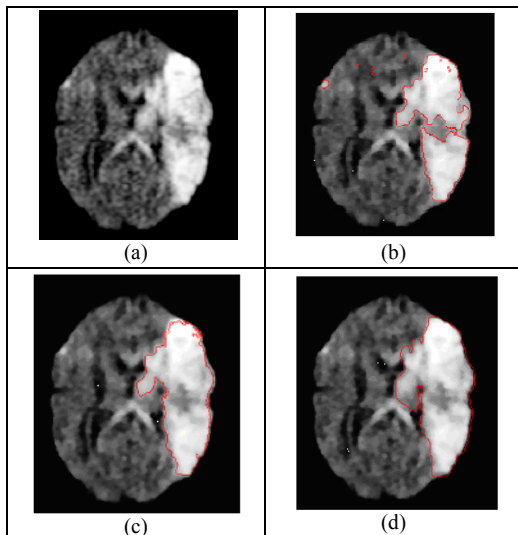


Fig 4. (a) Original image; (b) Injury detection by region intensity-based asymmetry detection; (c) Injury detection by our method; (d) ground-truth injuries.

Table 2. Results of MRI sequence for patient #A

| MRI#  | Total brain area (pixels) | Injury area ground-truth (pixels) | Percent injury | Injury area computed (pixels) | Error rate |
|-------|---------------------------|-----------------------------------|----------------|-------------------------------|------------|
| 1     | 1885                      | 0                                 | 0              | 0                             | 0          |
| 2     | 3271                      | 0                                 | 0              | 0                             | 0          |
| 3     | 4421                      | 0                                 | 0              | 0                             | 0          |
| 4     | 5583                      | 66                                | 1.18%          | 53                            | 27.3%      |
| 5     | 6707                      | 145                               | 2.16%          | 137                           | 8.97%      |
| 6     | 7839                      | 741                               | 9.45%          | 696                           | 7.29%      |
| 7     | 8667                      | 707                               | 8.16%          | 754                           | 6.65%      |
| 8     | 9472                      | 583                               | 6.15%          | 548                           | 9.43%      |
| 9     | 10166                     | 552                               | 5.43%          | 541                           | 3.07%      |
| 10    | 10013                     | 548                               | 5.47%          | 526                           | 6.39%      |
| 11    | 9089                      | 189                               | 2.08%          | 168                           | 16.4%      |
| 12    | 8154                      | 108                               | 1.32%          | 98                            | 10.2%      |
| 13    | 9444                      | 0                                 | 0              | 0                             | 0          |
| 14    | 8825                      | 0                                 | 0              | 0                             | 0          |
| 15    | 7019                      | 0                                 | 0              | 0                             | 0          |
| 16    | 7086                      | 0                                 | 0              | 0                             | 0          |
| Total | 117640                    | 3639                              | 3.09%          | 3452                          | 7.53%      |

## 4.2. Experimental Results

We run our algorithms on MRI sequences of two patients. An example slice and the result of each step are shown in Fig 1. Slices from patient #A and #B are shown in Fig 2 and Fig 3. As can be seen in the example of patient #A from Fig 2 (c) to (d), the normal asymmetric regions are eliminated by unsupervised classifier without any training phase or prior model, only using a 2-dimensional feature introduced in section 3.5. The final injury regions in Fig 2(d) are compared to the ground-truth injuries in 2(e), by finding the percentage of overlap and non-overlap area.

The percentage of non-overlap area, also called the false positive rate, determines the error rate, as shown in Table 2. Fig 3 also shows some example results from patient #B. The overall error rate of patient #A by our method is 7.53% shown in Table 2, and 9.14% for patient #B. Comparisons between Fig 2(d) and (e), also between Fig 3(d) and (e) show that most of the injuries can be successfully extracted with low error rate by our method. The error rate of non-overlapping area directly comes from the segmentation results. By searching better parameters of segmentation to improve the injury region boundary, the error rate can further be reduced. One of our future works will be focused on segmentation optimization by effective parameter searching. Table 2 provides statistical results of MRI sequence from patient #A. One challenging case in Fig 4 shows the successful detection of injury by our method in Fig 4(c), a better result compared to the result in Fig 4(b), which extracts asymmetric regions by directly comparing a region's intensity with its mirror region with respect to the symmetric axis. The error rate by our method in Fig 4(c) is 11.4%, compared to 27.6% by the method in Fig 4(b).

## 5. Conclusions

This paper provides a new injury detection method for brain MRIs. A symmetry-integrated image segmentation is applied to ensure that the symmetry property is preserved in the segmentation results. Kurtosis and skewness are used with a symmetry affinity matrix to extract potential asymmetric regions. An asymmetry grouping using 3D relaxation algorithm is combined to further refine the asymmetric regions. Brain injuries are finally extracted from asymmetric regions using an unsupervised classifier based on the Gaussian mixture model. Both qualitative and quantitative results on the data from the two patients show that the volume of the computed injury closely approximates the ground-truth. In the future we will evaluate the approach on larger scale of datasets.

**Acknowledgements:** The authors would like to thank Stephen Ashwal and Andre Obenaus of LLUMC for

providing us the MRI data that has been used in this paper. This research was supported in part by NSF grant 0641076.

## References

- [1] P. M. Birgani, M. Ashtiyani and S. Asadi, "MRI Segmentation Using Fuzzy C-means Clustering Algorithm Basis Neural Network," IEEE ICTTA, 2008.
- [2] Y. Kabir, M. Dojat, B. Scherrer, C. Garbay and F. Forbes, "Multimodal MRI segmentation of Ischemic Stroke Lesions," IEEE EMBS, 2007.
- [3] K. V. Leemput, F. Maes, D. Vandermeulen, A. Colchester and P. Suetens, "Automated Segmentation of Multiple Sclerosis Lesions by Model Outlier Detection," IEEE Trans. on Medical Imaging, Vol. 20, No. 8, August 2001.
- [4] M. B. Cuadra, C. Pollo, A. Bardera, O. Cuisenaire, J. Villemure and J. Thiran, "Atlas-Based Segmentation of Pathological MR Brain Images Using a Model of Lesion Growth," IEEE Trans. on Medical Imaging, Vol. 23, No. 10, October 2004.
- [5] G. Manana, E. Romero and F. Gonzalez, "A Grid Computing Approach to Subtraction Radiography," IEEE ICIP, 2006.
- [6] Z. Cao, X. Liu, B. Peng and Y. Moon, "DSA image registration based on multiscale Gabor Filters and Mutual Information," IEEE ICIA, 2005.
- [7] G. Loy and J. Eklundh, "Detecting Symmetry and Symmetric Constellations of Features," ECCV, 2006.
- [8] V. S. N. Prasad and B. Yegnanarayana, "Finding Axes of Symmetry From Potential Fields," IEEE Trans. on Image Processing, Vol. 13, No. 12, 2004.
- [9] Q. Du and I. Kopriva, "Automated Target Detection and Discrimination Using Constrained Kurtosis Maximization," Geoscience and Remote Sensing Letters, Vol. 5, No. 1, Jan. 2008.
- [10] A. Gupta, V. S. N. Prasad and L. S. Davis, "Extracting Regions of Symmetry," ICIP, 2005.
- [11] B. Bhanu and O. D. Faugeras, "Segmentation of Images Having Unimodal Distributions," IEEE Trans. on PAMI, 4(4), pp 408-419.
- [12] S. Saha and S. Bandyopadhyay, "MRI Brain Image Segmentation by Fuzzy Symmetry Based Genetic Clustering Technique," IEEE Congress on Evolutionary Computation, 2007.
- [13] F.P.G. Bergo, A.X. Falcao, C.L. Yasuda and F. Cendes, "FCD Segmentation Using Texture Asymmetry of MR-T1 Images of The Brain", ISBI, 2008.
- [14] N. Ray, R. Greiner and A. Murtha, "Using Symmetry to Detect Abnormalities in Brain MRI," Computer Society of India Communications, 31(19), pp 7-10, 2008.
- [15] I. N. Bankman, "Handbook of Medical Imaging Processing and Analysis," Academic Express, Series in Biomedical Engineering, 2000.